Clinical and Experimental Medicine (2018) 18:523–533
https://doi.org/10.1007/s10238-018-0509-2

ORIGINAL ARTICLE

MYLK promotes hepatocellular carcinoma progression through regulating cytoskeleton to enhance epithelial–mesenchymal transition

Jie Lin[1,2] · Yihui He[1,2] · Lingfeng Chen[1,2] · Xiaoyan Chen[1,2] · Shengbing Zang[3] · Wansong Lin[4,5]

Received: 31 December 2017 / Accepted: 24 May 2018 / Published online: 31 May 2018

Abstract

Myosin light chain kinase (MYLK) is found to catalyze the phosphorylation of myosin light chains (MLC) and regulate invasion and metastasis in some malignancies. However, there is little knowledge on the role of MYLK in hepatocellular carcinoma (HCC), and no studies have been conducted to investigate the mechanisms underlying MYLK-mediated promotion of HCC invasion and metastasis until now. In this study, we investigated the expression of MYLK in 50 pairs of human HCC and adjacent liver specimens. High MYLK expression was significantly correlated with aggressive clinicopathological features including tumor encapsulation, microvascular invasion and metastasis. In vitro assays showed that shRNA-induced MYLK knockdown significantly inhibited the wound-healing ability of HCC cells and the ability to migrate and invade through Matrigel. We next uncovered that MYLK knockdown resulted in a reduction in the number of F-actin stress fibers, disorganization of F-actin architectures and morphological alterations of HCC cells. Phosphorylated MLC, rather than total MLC, was found to be markedly reduced in response to downregulation of MYLK expression, and MYLK-regulated actin cytoskeleton through phosphorylating MLC in HCC cells. In addition, Western blotting assay revealed downregulation of the epithelial marker E-cadherin and upregulation of mesenchymal markers Vimentin, N-cadherin and Snail. Taken together, our findings indicate that MYLK promotes HCC progression by altering cytoskeleton to enhance epithelial–mesenchymal transition (EMT).

Keywords Myosin light chain kinase · Hepatocellular carcinoma · Cytoskeleton · Invasion and metastasis · Epithelial–mesenchymal transition

Abbreviations

MYLK	Myosin light chain kinase
HCC	Hepatocellular carcinoma
EMT	Epithelial–mesenchymal transition
MLC	Myosin light chains
IHC	Immunohistochemistry
shRNA	Short hairpin RNAs
qRT-PCR	Quantitative real-time PCR
NC	Negative control
SDS-PAGE	Sodium dodecyl sulfate polyacrylamide gel electrophoresis

✉ Wansong Lin
linwansong82@163.com

Jie Lin
sllinjie@163.com

Yihui He
heyihuitg@163.com

Lingfeng Chen
chenlingfeng2013@163.com

Xiaoyan Chen
slyycxy2013@163.com

Shengbing Zang
shengbingzang@163.com

[1] Department of Pathology, Fujian Provincial Hospital, Fuzhou 350001, China

[2] Shengli Clinical Medical College of Fujian Medical University, Fuzhou 350001, China

[3] Department of Pathology, The School of Basic Medical Sciences, Fujian Medical University, Fuzhou 350122, China

[4] Laboratory of Immuno-Oncology, Fujian Cancer Hospital and Fujian Medical University Cancer Hospital, No.420, Fuma Road, Jinan District, Fuzhou City 350014, Fujian Province, China

[5] Fujian Provincial Key Laboratory of Translational Cancer Medicine, Fuzhou 350014, China

IF Immunofluorescence
SD Standard deviation

Introduction

Cancer cell invasion and metastasis is a multistep process that begins with dissemination into surrounding tissues, then intravasates into and transits through the hematogenous and lymphatic systems, and finally extravasates and forms metastatic nodules at a distant site [1]. Each of these steps involves the change of cell motility, which is regulated by the remodeling of actin cytoskeletal structure [2]. Myosin light chain kinase (MYLK), encoded by the *mylk1* gene, is a calcium ion (Ca^{2+})/calmodulin (CaM)-dependent enzyme [3]. There are two types of protein products—isoforms derived from the human *mylk1* gene, including MYLK long isoform (L-MYLK) with a molecular weight of 210–220 kD and MYLK short isoform (S-MYLK) with 108–155 kD in molecular weight [4]. Both isoforms are found to catalyze the phosphorylation of myosin light chains (MLC), a key event that facilitates the association of myosin with F-actin and generates contractile force [5]. It has been shown that MYLK principally contributes to a variety of physiological processes that are related with myosin activation, such as cell adhesion, migration, division, invasion and metastasis [4, 6].

Aberrant MYLK expression has been reported to be involved in the malignant transformation of normal cells and affect migratory and invasive properties of tumor cells [7–11]. Previous studies have linked MYLK to the invasion and metastasis of multiple cancers, including lung cancer, colorectal cancer and breast cancer [8, 12–14]. In addition, MYLK was identified as a novel therapeutic target for hepatocellular carcinoma (HCC) [15]; however, the exact role of MYLK in human HCC progression remains unknown until now. The present study was, therefore, designed to examine the involvement of MYLK in human HCC progression and investigate the underlying mechanisms.

Materials and methods

Ethical approval

The study was approved by the Ethics Committee Review of Fujian Provincial Hospital (permission no.: K2017-05-004), and signed informed consent was obtained from all patients participating in the study, following a detailed description of the purpose of the study.

Patients and specimens

Fifty pairs of HCC and adjacent liver specimens (at least 2 cm away from the tumor, with no tumor detected as revealed by microscopy) were sampled from patients (42 males and 8 females, mean age 58 years) who underwent hepatic resection at Fujian Provincial Hospital (Fuzhou, China) during the period from January to December, 2016. The specimens were fixed in 10% neutral formalin, embedded in paraffin and cut into 3-μm sections for immunohistochemistry (IHC). Additionally, 10 pairs of fresh HCC and adjacent liver specimens (the same criteria as described above) were collected from 10 patients (7 males and 3 females, mean age 61 years) undergoing hepatic resection at Fujian Provincial Hospital (Fuzhou, China) between February and April, 2018. The specimens were frozen in liquid nitrogen immediately upon resection from the body, and then stored at − 80 °C for protein extraction. None of the patients received preoperative therapy. The diagnosis and identification of pathological factors of HCC were confirmed by two independent histopathologists. Patients' clinical records were carefully reviewed to capture the clinicopathological features

IHC

Sections were stained using the EliVision™ plus two-step method (EliVision™ Super KIT9922; Fuzhou Maixin Biotech. Co., Ltd.; Fuzhou, China) and incubated in mouse anti-MYLK monoclonal antibody (MABT194,1:50 dilution; Millipore, Billerica, MA, USA), while the fibrocytes in the mesenchyme, in which MYLK is not expressed, served as an internal negative control [16]. Two pathologists, blinded to clinicopathological data, independently evaluated the immunostained sections. Staining intensity was scored as follows: 0, negative; 1, pale yellow; 2, medium yellow; and 3, tawny. The proportion of positive-stained cells was scored as follows: 0, ≤ 10%; 1, 11–25%; 2, 26–50%; 3, 51–75%; and 4, ≥ 76%. We then multiplied intensity scores by proportion scores to obtain total scores. Cases with a total score of 0–3 were defined as low MYLK expression and those with a total score of 4–12 as high expression.

Cell lines and culture

Human HCC LM3, MHCC97H and MHCC97L cell lines were purchased from the Liver Cancer Institute of Fudan University (Shanghai, China). The Sk-Hep1 and HepG2 cell lines were purchased from the American Tissue Culture Collection (Manassas, VA, USA). The SMMC7721 cell line was purchased from the Cell Bank of the Chinese

Academy of Sciences (Shanghai, China). The Huh7 cell line was maintained in our laboratory. All cell lines were maintained in DMEM (Gibco; Grand Island, NY, USA) supplemented with 10% fetal bovine serum (FBS; Gibco; Grand Island, NY, USA), 100 U/ml penicillin (Gibco; Grand Island, NY, USA) and 100 mg/ml streptomycin (Gibco; Grand Island, NY, USA) at 37 °C containing 5% CO_2.

Cell transfection

Three short hairpin RNAs (shRNA) targeting MYLK (MYLK-shRNA) and a negative control (shControl) were synthesized by Genechem Co., Ltd. (Shanghai, China) (Table 1) and cloned into the lentiviral vector GV248 (Genechem Co., Ltd.; Shanghai, China). Using the packaging plasmids pHelper 1.0 and pHelper 2.0 (Genechem Co., Ltd.; Shanghai, China), three lentivirus types expressing shRNA were generated and used simultaneously to infect LM3 and MHCC97H cells. After 72-h infection, infected cells were cultured in the medium containing 2 μg/ml puromycin (Gibco; Grand Island, NY, USA) to select stable MYLK-knockdown cells. Stable MYLK-silenced cells were designated LM3/LV-shMYLK and MHCC97H/LV-shMYLK, whereas control cells we named LM3/LV-shctrl and MHCC97H/LV-shctrl. MYLK expression in all stable cell lines was verified by Western blotting.

Quantitative real-time PCR (qPCR) assay

Total RNA was extracted using the TRIzol reagent (Invitrogen; Carlsbad, CA, USA) and reversely transcribed into cDNA using Superscript III Reverse Transcriptase (Invitrogen). qPCR assay was performed using the SYBR Master Mix (Takara; Shiga, Japan) on an ABI7500 real-time PCR system (Applied Biosystems; Foster City, CA, USA), and the primer sequences used are listed in Table 1. Relative gene expression was calculated using the $2^{-\Delta\Delta Ct}$ method.

Western blotting

Total protein was extracted from fresh specimens and cell lysates and separated by sodium dodecyl sulfate polyacrylamide gel electrophoresis (SDS-PAGE) on 10% gels. The bands were then transferred onto PVDF membranes (Millipore; Billerica, MA, USA) and incubated with mouse anti-MYLK monoclonal antibody (MABT194; Millipore, Billerica, MA, USA; 1:1000 dilution) overnight at 4 °C, while GAPDH (ab8245; Abcam, Camridge, MA, USA; 1:5000) served as a loading control. PVDF membranes transferred with cell proteins were also incubated with rabbit anti-MLC monoclonal antibody (#8505; Cell Signaling Technology, Beverly, MA, USA; 1:1000 dilution), rabbit anti-phospho-MLC (Thr18/Ser19) polyclonal antibody (#3674; Cell Signaling Technology Beverly, MA, USA; 1:1000 dilution), rabbit anti-phospho-MLC (Ser19) polyclonal antibody (#3671; Cell Signaling Technology Beverly, MA, USA; 1:1000 dilution), rabbit anti-E-cadherin monoclonal antibody (ab40772; Abcam, Cambridge, UK; 1:10000 dilution), rabbit anti-Vimentin monoclonal antibody (#5741; Cell Signaling Technology, Beverly, MA, USA; 1:1000 dilution), rabbit anti-Snail monoclonal antibody (#3879; Cell Signaling Technology, Beverly, MA, USA; 1:1000 dilution) and rabbit anti-β-catenin monoclonal antibody (#8480; Cell Signaling Technology, Beverly, MA, USA; 1:1000 dilution) overnight at 4 °C, with GAPDH as a loading control. Then, the PVDF membranes were incubated with the HRP-conjugated IgG secondary antibody (Cell Signaling Technology, Beverly, MA, USA). Blots were visualized using an enhanced chemiluminescence kit (Thermo Fisher; Waltham, MA, USA) and detected using the QuantityOne software (Bio-Rad; Hercules, CA, USA).

Table 1 Primer sequences

Primers	Uses	Sequences
MYLK-shRNA1	Targeting the conservative region (5586–5604 bp) of MYLK mRNA	5′- CGGGAACTGCTCTTTAATT -3′
MYLK-shRNA2	Targeting the conservative region (5273–5291 bp) of MYLK mRNA	5′- TGTCCTCTATGGCAATGAT -3′
MYLK-shRNA3	Targeting the conservative region (6777–6795 bp) of MYLK mRNA	5′- TACCTTATGGGTTCCATAT -3′
shControl	Negative control of MYLK-shRNA	5′- TTCTCCGAACGTGTCACGT -3′
MYLK-F	Verifying *MYLK*-knockdown clones	5′- CGACGAGGCATTCGATGAGA -3′
MYLK-R		5′- AGTTTTTCTGCATTGAGCGGG -3′
GAPDH-F	Control of the MYLK primer	5′- GCCGCATCTTCTTTTGCGTC -3′
GAPDH-R		5′- TACGACCAAATCCGTTGACTCC -3′

Wound-healing assay

HCC cells were cultured in two wells of the Culture-Insert (Ibidi; Munich, Germany). If both wells were filled with adherent cells, a wound at approximately 500 μm was created by gently removing the Culture-Insert. Then, cells were maintained in DMEM supplemented with 10% FBS and antibiotics. The cells were observed, and images were captured 0, 24 and 48 h after the wound creation.

Transwell migration and invasion assays

Migration and invasion assays were performed using uncoated or Matrigel-coated (Corning; Corning, NY, USA) transwell culture chambers (Millipore; Billerica, MA, USA) following the manufacturer's instructions. The Matrigel membrane was stained using crystal violet, and migrating or invading cells were counted in 5 randomly selected visual fields at 200× magnification. Each experiment was independently repeated in triplicate.

Immunofluorescence (IF) staining

LM3 and MHCC97H cells stably infected with MYLK-shRNA or control lentivirus vector were grown on glass coverslips. Cells were fixed in 4% paraformaldehyde, permeabilized with 0.5% Triton X-100 and incubated with Alexa Fluor 488 phalloidin (Invitrogen; Carlsbad, CA, USA). Then, the cell nuclei were counterstained using fluoroshield mounting medium with DAPI (Abcam; Camridge, MA, USA). The slides were examined under a fluorescence microscope (Leica; Wetzlar, Germany).

Statistical analysis

All measurement data were expressed as mean ± standard deviation (SD), and all count data were presented as proportions. Differences of means between groups were tested for statistical significance with Student's *t*-test, while comparisons of proportions were done using Chi-square test. Enumerated data were compared using the Kruskal–Wallis *H* (K) test. All statistical analyses were conducted with the statistical software SPSS version 19.0 (SPSS, Inc.; Armonk, NY, USA), and a *P* value of < 0.05 was indicative of statistical significance.

Table 2 Comparison of MYLK expression between HCC and adjacent liver specimens

Specimens	MYLK expression (*n*)		MYLK high expression (%)	*Z* value	*P* value
	High	Low			
HCC specimens	31	19	62	−3.500	0.000
Adjacent liver specimens	17	33	34		

Results

Elevated MYLK expression is detected in HCC specimens and correlated with tumor metastasis

IHC was performed to assess MYLK expression in 50 paired HCC and adjacent liver specimens. We found that MYLK was localized in the cytoplasm, and high MYLK expression was detected in 31 of the 50 (62%) HCC specimens compared with 17 of the 50 (34%) corresponding adjacent specimens ($Z = -3.5$, $P = 0$) (Table 2, Fig. 1a–e). Then, we evaluated the correlation between MYLK expression and clinicopathological features of HCC patients. High MYLK expression was found to be positively correlated with microvascular invasion ($P = 0.017$) and metastasis ($P = 0.034$) and may be associated with tumor encapsulation ($P = 0.059$) (Table 3). Next, Western blotting was employed to determine MYLK expression in additional 10 paired HCC and adjacent liver specimens. All 10 pairs of HCC and adjacent liver specimens expressed S-MYLK and 2 pairs expressed L-MYLK mildly. Compared with the adjacent liver specimens, S-MYLK expression was upregulated in 6 HCC specimens and downregulated in one specimen. In addition, similar S-MYLK expression profile was seen in another 3 pairs of HCC and adjacent liver specimens (Fig. 1f). Taken together, our data indicate that HCC predominantly expresses S-MYLK, which contributes to HCC progression and acts as a promoter of HCC metastasis.

Knockdown of MYLK expression inhibits HCC cell motility and invasiveness

To investigate the function of MYLK *in vitro*, Western blotting was performed to determine MYLK protein expression in seven HCC cell lines. S-MYLK was found to be expressed in all seven cell lines, and higher S-MYLK expression was detected in the high-metastatic SK-Hep1, LM3, MHCC97H and MHCC97L cell lines than in the low-metastatic HepG2, Huh7 and SMMC7721 cell lines. Interestingly, no L-MYLK expression was detected in high-metastatic SK-Hep1, LM3 or MHCC97H cells, while low L-MYLK expression was

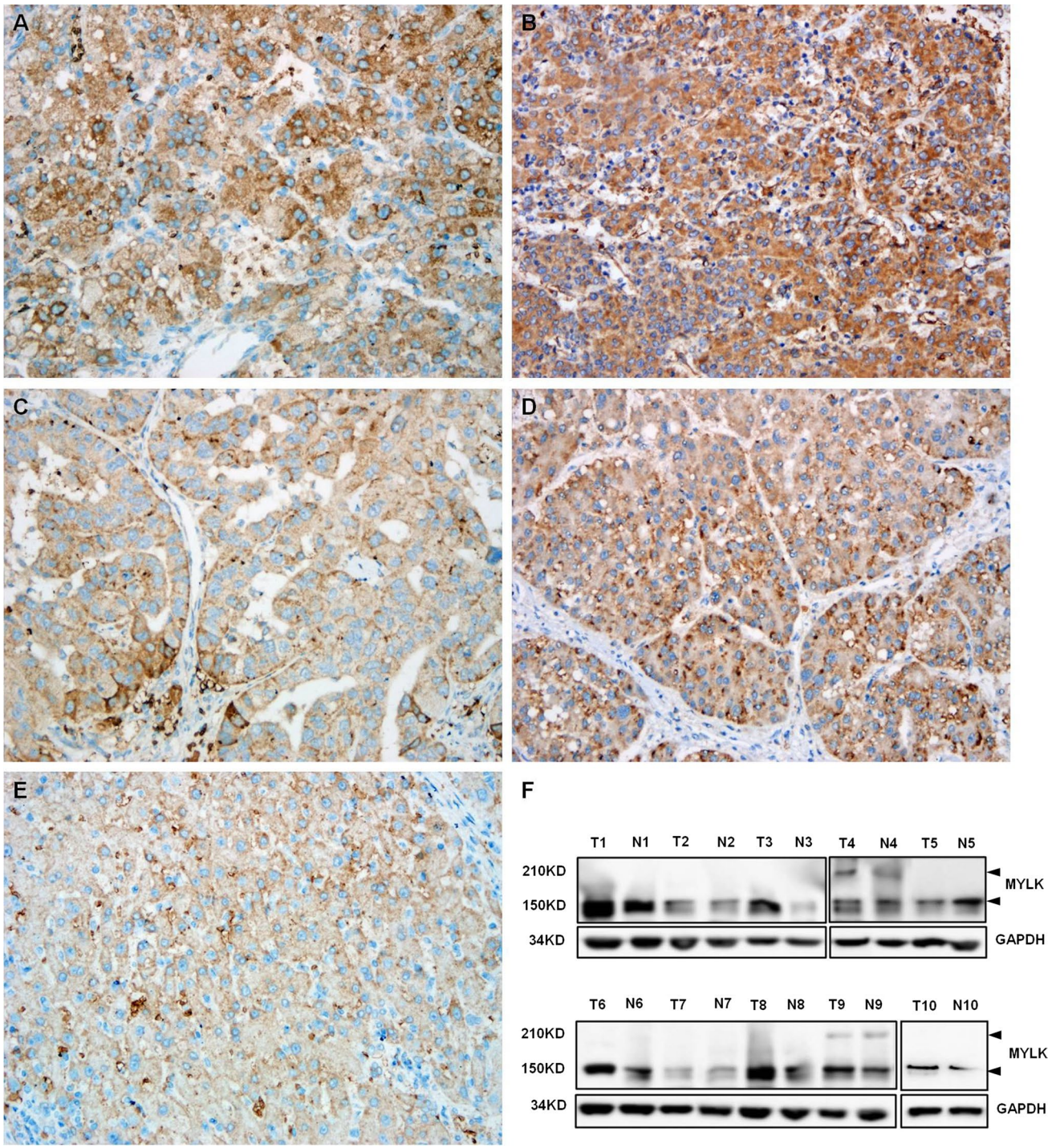

Fig. 1 MYLK expression is upregulated in HCC specimens. Immunohistochemical analysis is performed to detect MYLK expression in 50 pairs of HCC and adjacent liver specimens. MYLK expression is higher in HCC specimens (**a** to **d**) than in adjacent liver specimens (**e**). **a** and **b** The staining intensity is tawny; **c** and **d** the staining intensity is medium yellow; **f** Western blotting analysis is performed to detect the MYLK expression in additional 10 pairs of HCC and adjacent liver specimens. HCC specimens are found to predominantly express the MYLK short isoform (S-MYLK). The S-MYLK expression is upregulated in 6 HCC specimens and downregulated in one specimen. Similar expression profile of S-MYLK is seen in another 3 pairs of HCC and adjacent liver specimens

Table 3 Association of MYLK expression with clinicopathological characteristics in HCC patients

Clinicopathological features	*n*	MYLK expression		High MYLK expression (%)	χ^2 value	*P* value
		High ($n=31$)	Low ($n=19$)			
Sex						
Female	8	4	4	50	0.57	0.45
Male	42	27	15	64.29		
Age (years)						
≤ 60	35	23	12	65.71	0.669	0.413
>60	15	8	7	53.33		
Serum AFP (ng/ml)						
≤ 252	17	10	7	58.82	0.108	0.742
>252	33	21	12	63.64		
HBsAg						
Negative	7	5	2	71.43	0.301	0.583
Positive	43	26	17	60.47		
Liver cirrhosis						
Absence	14	11	3	78.57	2.221	0.136
Presence	36	20	16	55.56		
Tumor number						
Single	46	30	16	65.22	2.476	0.116
Multiple	4	1	3	25		
Maximal tumor size (cm)						
≤ 3	7	5	2	71.43	0.301	0.583
>3	43	26	17	60.47		
Edmondson–Steiner grade						
I and II	31	21	10	67.74	1.119	0.29
III and IV	19	10	9	52.63		
Tumor encapsulation						
Absence	23	11	12	47.83	3.559	0.059
Presence	27	20	7	74.07		
Microvascular invasion						
Absence	26	12	14	46.15	5.658	0.017
Presence	24	19	5	79.17		
Metastasis						
Absence	30	15	15	50	4.492	0.034
Presence	20	16	4	80		

seen in low-metastatic HepG2, Huh7 and SMMC7721 cells. Although MHCC97L cells also expressed L-MYLK, the level was extremely weak (Fig. 2a). It is suggested that MYLK, notably S-MYLK, may play a causal role in HCC invasion and metastasis. Therefore, our studies focused on the effect of S-MYLK on HCC cell function. LM3 and MHCC97H cells were selected to generate stably transfected HCC cell lines with MYLK knockdown (Fig. 2b), and the motility and invasiveness of these stably transfected cells were examined using wound-healing and transwell assays. Downregulation of MYLK expression was fount to significantly inhibit the wound-healing ability of LM3 and MHCC97H cells and decrease the number of cells migrating through or invading into the Matrigel (Fig. 3). Our data indicate that shRNA-induced knockdown of MYLK inhibits HCC cell motility and invasiveness *in vitro*.

MYLK affects cytoskeleton organization through MLC phosphorylation

To evaluate the effect of MYLK on the cytoskeletal organization, F-actin was labeled with the Alexa Fluor 488 phalloidin in LM3 and MHCC97H cells. We observed F-actin stress fibers and well-organized F-actin bundles in non-transfected cells and shControl-transfected cells. Conversely, shRNA-induced MYLK knockdown led to a reduction in the number of F-actin stress fibers and disorganized F-actin architecture in LM3 and MHCC97H cells

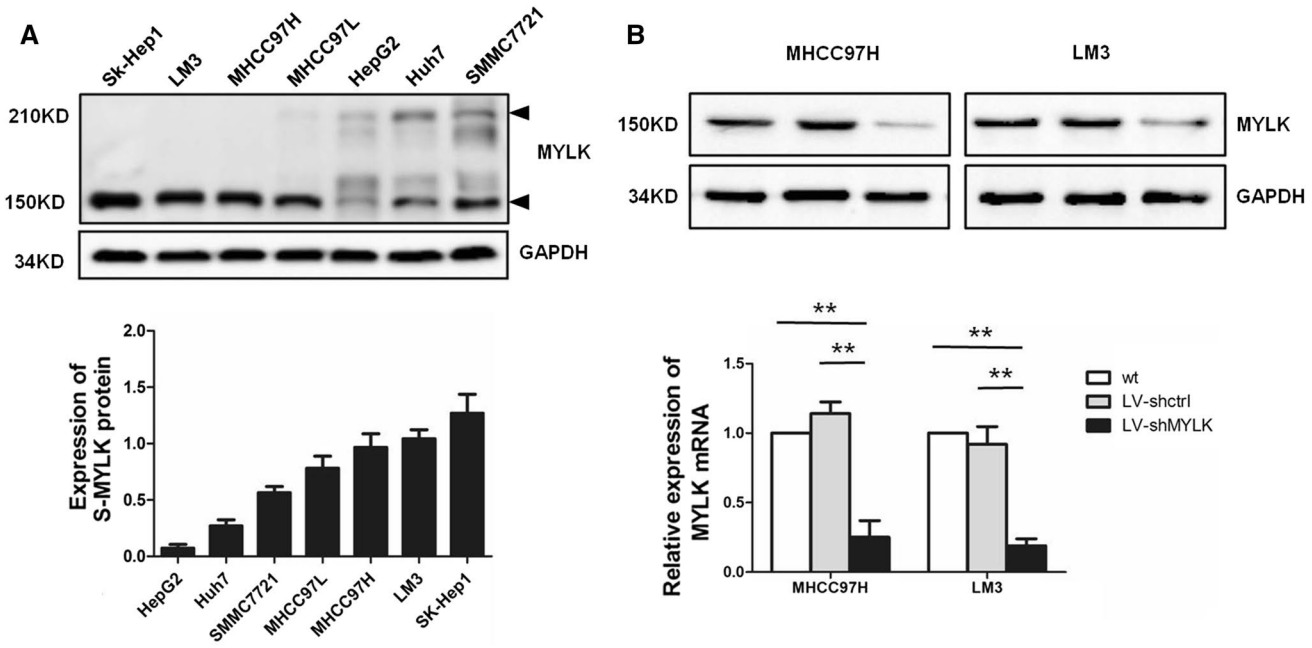

Fig. 2 Generation of stably transfected MYLK-knockdown HCC cell lines. a Western blotting analysis of MYLK expression in seven human HCC cell lines, and the expression of the MYLK short isoform is higher in the high-metastatic SK-Hep1, LM3, MHCC97H and MHCC97L cell lines than in the low-metastatic HepG2, Huh7 and SMMC7721 cell lines; **b** Western blotting and qPCR assays detect MYLK expression in stably transfected HCC cell lines. ** $P < 0.01$

(Fig. 4a). These results demonstrate that MYLK affects the F-actin cytoskeleton organization.

In order to investigate the molecular mechanisms underlying the MYLK-mediated cytoskeletal organization, Western blotting was performed to detect MLC expression. There was no alteration seen in total MLC expression; however, the level of both di-phosphorylated MLC and mono-phosphorylated MLC (Ser19) expressions was remarkably reduced in LM3 or MHCC97H cells with MYLK knockdown (Fig. 4b). Our data suggest that MYLK may alter cytoskeleton through MLC phosphorylation.

Knockdown of MYLK expression reverses epithelial–mesenchymal transition (EMT) in HCC cells

To assess the effect of MYLK on EMT in HCC cells, Western blotting was performed to determine the expression of EMT biomarkers. Knockdown of MYLK expression was found to result in elevated expression of the epithelial marker E-cadherin in both LM3 and MHCC97H cells; however, MYLK downregulation inhibited the expression of mesenchymal markers Vimentin, N-cadherin and Snail (Fig. 5). These results demonstrate that knockdown of MYLK expression reverses EMT in HCC cells.

Discussion

Cancer cell migration and invasion are essential features of epithelial-originated carcinomas in the process of cancer progression [17]. To discriminate from the primary lesion, cancer cells regulate their cytoskeletal structures to increase their motility, which is implicated in the process of EMT [18]. In this study, we firstly detected elevated MYLK expression in clinical HCC specimens and elevated MYLK expression was found to be significantly associated with aggressive clinicopathological features of HCC. In addition, this is the report demonstrating that MYLK promotes HCC cell migration and invasion through remodeling actin cytoskeletal structures to trigger EMT. It is therefore considered that MYLK may be a promising biomarker for diagnosis and a potential therapeutic target of HCC.

Previous studies have shown that carcinogenesis and malignant progression are associated with altered MYLK expression in multiple cancers [11, 14, 19–21]. High MYLK expression was detected in non-small-cell lung cancer (NSCLC) with lymphatic metastasis relative to without lymphatic metastasis, and stages III and IV NSCLC exhibited higher MYLK expression than stages I and II [8]. Similarly, downregulation of endogenous MYLK expression, or ML-7, an inhibitor of MYLK, significantly inhibited the migration of human colon adenocarcinoma RKO cells [13]. However, an opposite role of

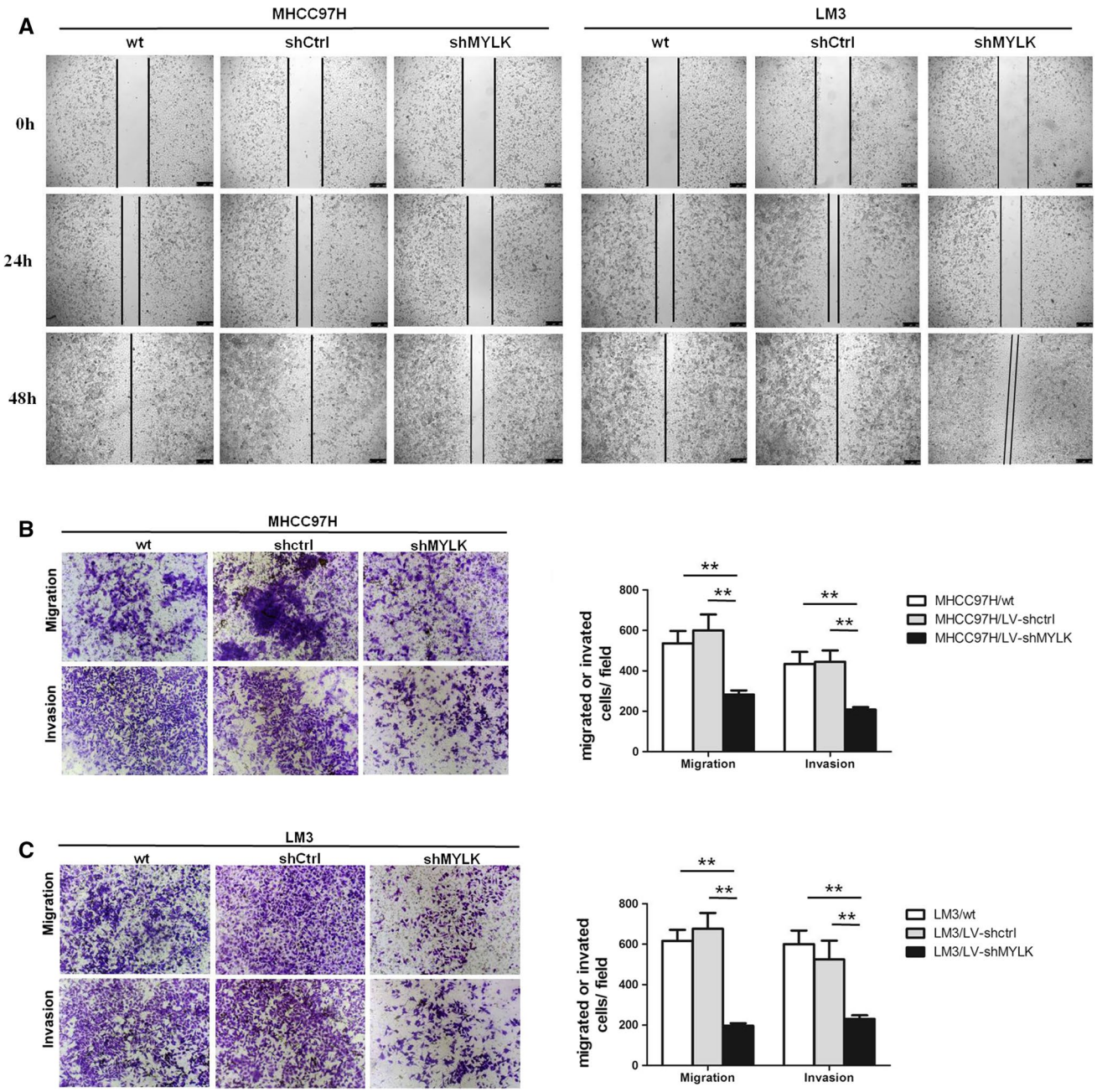

Fig. 3 Knockdown of MYLK expression inhibits HCC cell motility and invasiveness. **a** Effect of MYLK knockdown on HCC cell migration assessed by the wound-healing assay. The margin of the HCC cells is marked by the vertical line, and HCC cells migrate and move into the wounded areas 24 and 48 h after the wound creation. The distance between the two vertical lines represent the cell migratory capacity, and a less distance indicates a stronger HCC cell migratory ability; **b** and **c** effect of MYLK knockdown on HCC cell migration and invasion evaluated by the transwell assays. ** $P < 0.01$

MYLK was reported in breast cancer cell metastasis, and MYLK downregulation correlated with poor prognosis of breast cancer patients positive for HER2 [13]. In addition, MYLK was detected to be overexpressed in diethylnitrosamine (DENA)-induced HCC rats [13]. To the best of our knowledge, however, there is no knowledge on the role of MYLK in human HCC to date.

In the present study, we detected higher MYLK expression in HCC specimens than in the matched adjacent liver specimens, and MYLK upregulation was correlated with aggressive clinicopathological features including microvascular invasion and metastasis. Western blotting analysis confirmed that HCC and adjacent liver specimens mainly expressed S-MYLK. Consistently, higher MYLK

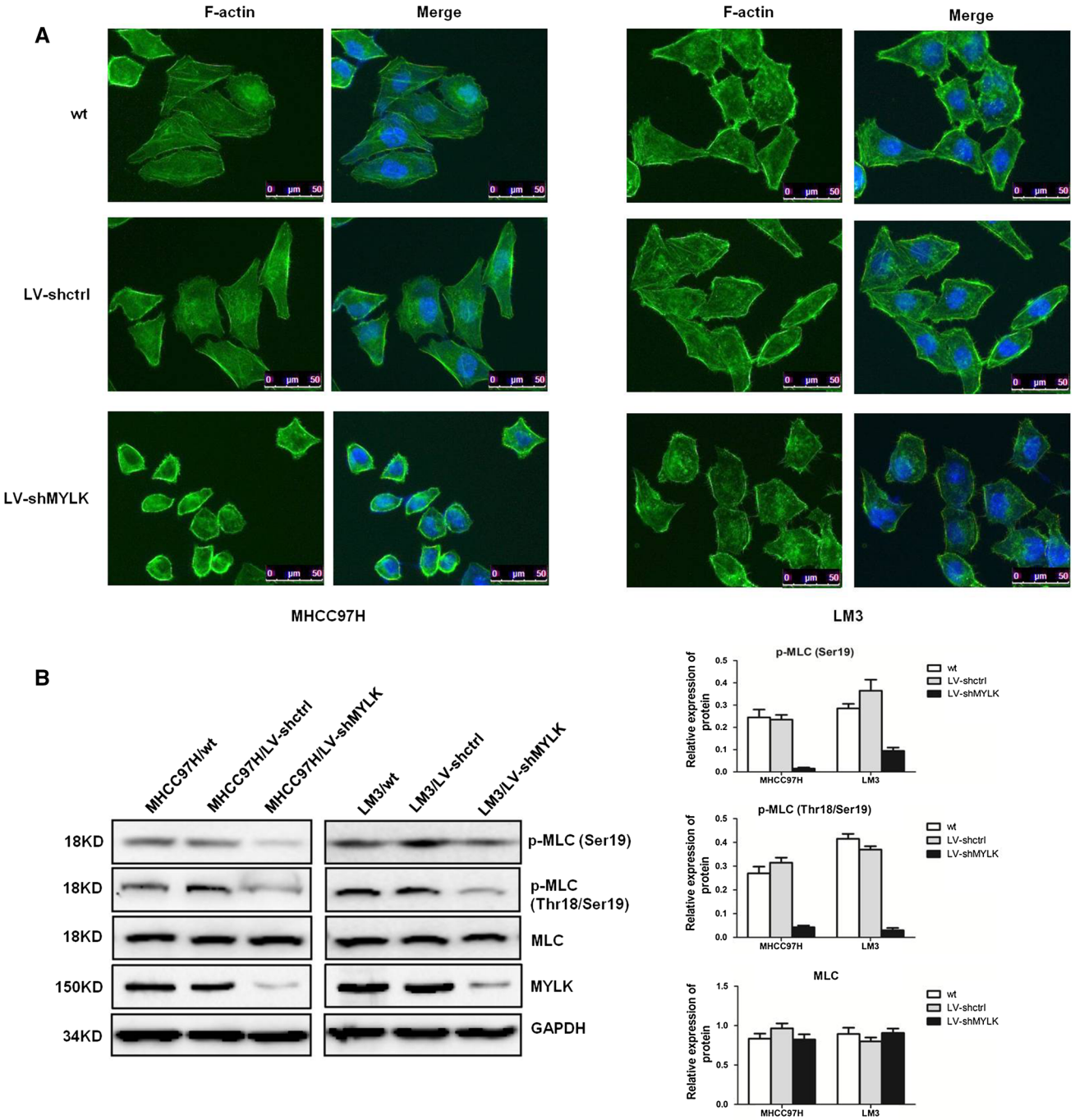

Fig. 4 Knockdown of MYLK expression affects cytoskeleton organization through phosphorylation of MLC. **a** MYLK knockdown results in a decrease in the number of F-actin stress fibers and disorganization of F-actin architectures in LM3 and MHCC97H cells; **b** Western blotting analysis reveals a clear-cut reduction in both the di-phosphorylated MLC (Thr18/Ser19) and mono-phosphorylated MLC (Ser19) expressions but no alteration of total MLC expression in LM3 or MHCC97H cells with MYLK knockdown

expression, notably S-MYLK, was seen in high-metastatic SK-Hep1, LM3, MHCC97H and MHCC97L cell lines than in low-metastatic HepG2, Huh7 and SMMC7721 cell lines, which is inconsistent with previous findings that untransformed breast epithelial cell lines and some breast cancer cell lines expressed L-MYLK [14]. It is speculated that such a difference may be attributed to the tissue-specific distribution of MYLK isoforms [4]. In addition, *in vitro* functional experiments showed that MYLK knockdown inhibited the migration and invasion of HCC cells. Taken together, our data indicate that MYLK plays a critical role in increasing HCC cell motility and promoting HCC progression.

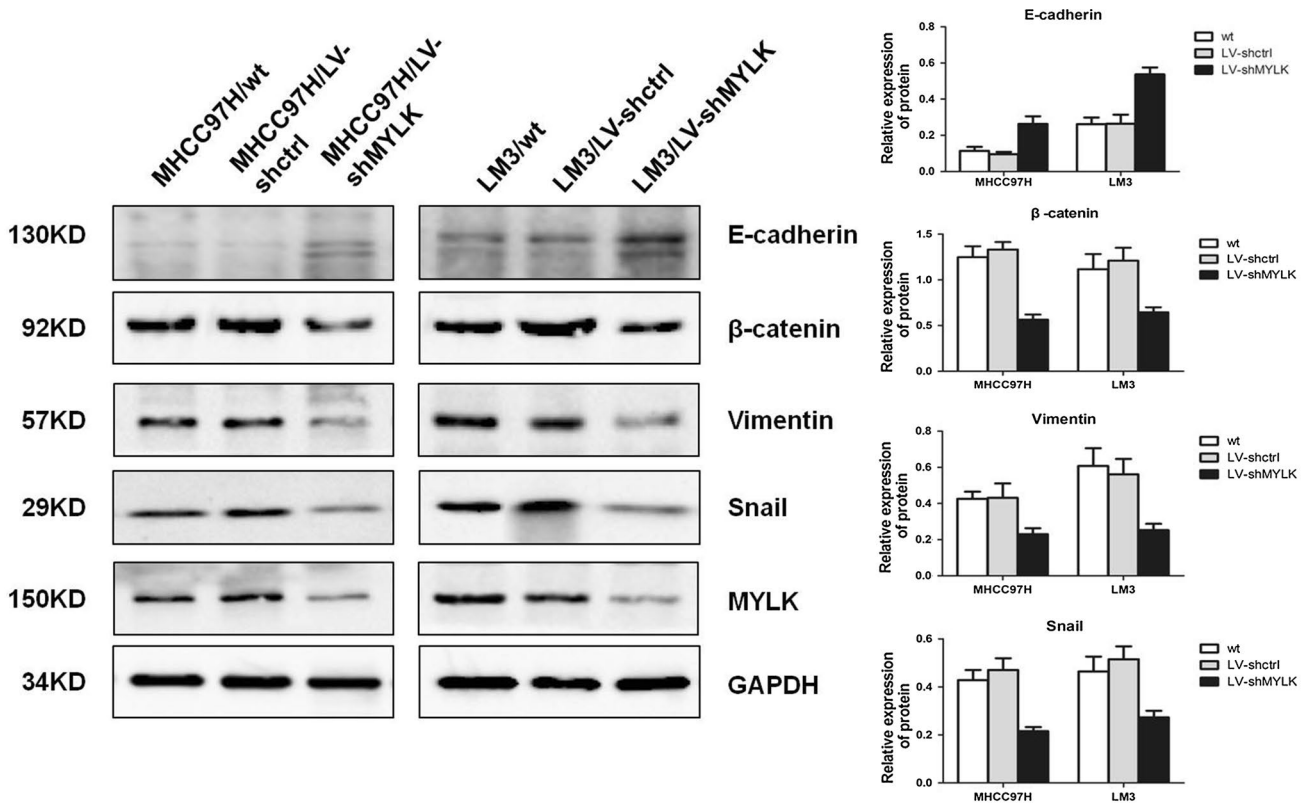

Fig. 5 Knockdown of MYLK expression reverses epithelial–mesenchymal transition (EMT) of HCC cells. Western blotting is employed to determine the expression of EMT biomarkers, and knockdown of MYLK expression results in an increase in E-cadherin expression and a decrease in Vimentin, N-cadherin and Snail expression in both LM3 and MHCC97H cells

Cell motility, which is important for cancer cell invasion and metastasis, is driven by cycles of actin polymerization, cell adhesion and actin–myosin contraction [22, 23]. Actin–myosin contraction is found to result in morphological remodeling of cancer cells and reorganization of extracellular matrix that facilitates cell movement [22, 23]. MLC phosphorylation, which is mediated by MYLK, is a key factor for regulating actin–myosin contraction [23, 24]. MYLK has been reported to affect cancer cytoskeleton [12]. Depletion of MYLK reduced the invadopodia formation of breast cancer cells and inhibited the invasive potential of cancer cells [12]. In addition, loss of MYLK was reported to result in alteration of cell–cell and cell–matrix adhesion [14]. In this study, shRNA-induced MYLK knockdown led to a decrease in the number of F-actin stress fibers, disorganization of F-actin architectures and morphological alteration of HCC cells. Furthermore, phosphorylated MLC, rather than total MLC, was remarkably reduced in response to down-regulation of MYLK expression. Our data demonstrate that MYLK may regulate actin cytoskeleton through phosphorylation of MLC.

EMT is an essential process for cancer cells to acquire migratory and invasive potential that is involved in cytoskeleton reorganization [25]. After discovering the role of MYLK in HCC progression and HCC cell actin cytoskeleton, it is hypothesized that MYLK may promote EMT in HCC. To test the hypothesis, we detected the expression of key EMT biomarkers [26], and knockdown of MYLK expression resulted in elevated expression of the epithelial marker E-cadherin and a reduction in the expression of mesenchymal markers Vimentin, N-cadherin and Snail. These results supported our hypothesis and suggest that MYLK promotes EMT in HCC cells.

Conclusions

In summary, the results of the present study demonstrate that high MYLK increases HCC cells aggression and promotes HCC progression. In addition, MYLK improves the migratory and invasive ability of HCC cells by altering cytoskeleton to enhance EMT.

Acknowledgements This study was funded by the National Natural Science Foundation of China (Grant Number: '81301444'), the Special Fund of Fujian Provincial Department of Finance (Grant Number: '2014-1262') and the Research Talent Training Program of Fujian Provincial Health and Family Planning Commission (Grant Number: '2017-ZQN-14').

Compliance with ethical standards

Conflict of interest The authors declare that they have no conflict of interest.

Ethical approval All procedures performed in studies involving human participants were in accordance with the ethical standards of the institutional and/or national research committee and with the 1964 Helsinki Declaration and its later amendments or comparable ethical standards.

Informed consent Informed consent was obtained from all individual participants included in the study.

References

1. Hanahan D, Weinberg RA. Hallmarks of cancer: the next generation. Cell. 2011;144(5):646–74. https://doi.org/10.1016/j.cell.2011.02.013.
2. Kelley LC, Shahab S, Weed SA. Actin cytoskeletal mediators of motility and invasion amplified and overexpressed in head and neck cancer. Clin Exp Metas. 2008;25(4):289–304. https://doi.org/10.1007/s10585-008-9154-6.
3. Cui C, Merritt R, Fu L, Pan Z. Targeting calcium signaling in cancer therapy. Acta pharmaceutica Sinica B. 2017;7(1):3–17. https://doi.org/10.1016/j.apsb.2016.11.001.
4. Khapchaev AY, Shirinsky VP. Myosin Light Chain Kinase MYLK1: anatomy, Interactions, Functions, and Regulation. Biochem Biokhimiia. 2016;81(13):1676–97. https://doi.org/10.1134/S000629791613006X.
5. Stull JT, Tansey MG, Tang DC, Word RA, Kamm KE. Phosphorylation of myosin light chain kinase: a cellular mechanism for Ca2+ desensitization. Mol Cell Biochem. 1993;127–128:229–37.
6. Park J, Kim DH, Kim HN, Wang CJ, Kwak MK, Hur E, et al. Directed migration of cancer cells guided by the graded texture of the underlying matrix. Nat Mater. 2016;15(7):792–801. https://doi.org/10.1038/nmat4586.
7. Cui WJ, Liu Y, Zhou XL, Wang FZ, Zhang XD, Ye LH. Myosin light chain kinase is responsible for high proliferative ability of breast cancer cells via anti-apoptosis involving p38 pathway. Acta Pharmacol Sin. 2010;31(6):725–32. https://doi.org/10.1038/aps.2010.56.
8. Tan X, Chen M. MYLK and MYL9 expression in non-small cell lung cancer identified by bioinformatics analysis of public expression data. Tumour biology : the journal of the International Society for Oncodevelopmental Biology and Medicine. 2014;35(12):12189–200. https://doi.org/10.1007/s13277-014-2527-3.
9. Leveille N, Fournier A, Labrie C. Androgens down-regulate myosin light chain kinase in human prostate cancer cells. J Steroid Biochem Mol Biol. 2009;114(3–5):174–9. https://doi.org/10.1016/j.jsbmb.2009.02.002.
10. Chen L, Su L, Li J, Zheng Y, Yu B, Yu Y, et al. Hypermethylated FAM5C and MYLK in serum as diagnosis and pre-warning markers for gastric cancer. Dis Mark. 2012;32(3):195–202. https://doi.org/10.3233/DMA-2011-0877.
11. Choi C, Kwon J, Lim S, Helfman DM. Integrin beta1, myosin light chain kinase and myosin IIA are required for activation of PI3 K-AKT signaling following MEK inhibition in metastatic triple negative breast cancer. Oncotarget. 2016;7(39):63466–87. https://doi.org/10.18632/oncotarget.11525.
12. Sundararajan V, Gengenbacher N, Stemmler MP, Kleemann JA, Brabletz T, Brabletz S. The ZEB1/miR-200c feedback loop regulates invasion via actin interacting proteins MYLK and TKS5. Oncotarget. 2015;6(29):27083–96. https://doi.org/10.18632/oncotarget.4807.
13. Zuo L, Yang X, Lu M, Hu R, Zhu H, Zhang S, et al. All-Trans Retinoic Acid Inhibits Human Colorectal Cancer Cells RKO Migration via Downregulating Myosin Light Chain Kinase Expression through MAPK Signaling Pathway. Nutr Cancer. 2016;68(7):1225–33. https://doi.org/10.1080/01635581.2016.1216138.
14. Kim DY, Helfman DM. Loss of MLCK leads to disruption of cell-cell adhesion and invasive behavior of breast epithelial cells via increased expression of EGFR and ERK/JNK signaling. Oncogene. 2016;35(34):4495–508. https://doi.org/10.1038/onc.2015.508.
15. Zhang X, Yu H. Matrine inhibits diethylnitrosamine-induced HCC proliferation in rats through inducing apoptosis via p53, Bax-dependent caspase-3 activation pathway and down-regulating MLCK overexpression. Iran J Pharm Res IJPR. 2016;15(2):491–9.
16. Blue EK, Goeckeler ZM, Jin Y, Hou L, Dixon SA, Herring BP, et al. 220- and 130-kDa MLCKs have distinct tissue distributions and intracellular localization patterns. Am J Physiol Cell Physiol. 2002;282(3):C451–60. https://doi.org/10.1152/ajpcell.00333.2001.
17. Yokota J. Tumor progression and metastasis. Carcinogenesis. 2000;21(3):497–503.
18. Iwatsuki M, Mimori K, Yokobori T, Ishi H, Beppu T, Nakamori S, et al. Epithelial-mesenchymal transition in cancer development and its clinical significance. Cancer Sci. 2010;101(2):293–9. https://doi.org/10.1111/j.1349-7006.2009.01419.x.
19. Yu HJ, Serebryannyy LA, Fry M, Greene M, Chernaya O, Hu WY, et al. Tumor Stiffness Is Unrelated to Myosin Light Chain Phosphorylation in Cancer Cells. PLoS ONE. 2013;8(11):e79776. https://doi.org/10.1371/journal.pone.0079776.
20. Zou DB, Wei X, Hu RL, Yang XP, Zuo L, Zhang SM, et al. Melatonin inhibits the migration of colon cancer RKO cells by down-regulating myosin light chain kinase expression through cross-talk with p38 MAPK. Asian Pacific journal of cancer prevention : APJCP. 2015;16(14):5835–42.
21. Wang B, Yan Y, Zhou J, Zhou Q, Gui S, Wang Y, Wang Y. A novel all-trans retinoid acid derivatives inhibits the migration of breast cancer cell lines MDA-MB-231 via myosin light chain kinase involving p38-MAPK pathway. Biomed Pharmacother. 2013;67(5):357–62. https://doi.org/10.1016/j.biopha.2013.03.016.
22. Yilmaz M, Christofori G. Mechanisms of motility in metastasizing cells. Mol Cancer Res MCR. 2010;8(5):629–42. https://doi.org/10.1158/1541-7786.MCR-10-0139.
23. Olson MF, Sahai E. The actin cytoskeleton in cancer cell motility. Clin Exp Metas. 2009;26(4):273–87. https://doi.org/10.1007/s10585-008-9174-2.
24. Gross SR. Actin binding proteins: their ups and downs in metastatic life. Cell Adhes Migr. 2013;7(2):199–213. https://doi.org/10.4161/cam.23176.
25. Yilmaz M, Christofori G. EMT, the cytoskeleton, and cancer cell invasion. Cancer Metastasis Rev. 2009;28(1–2):15–33. https://doi.org/10.1007/s10555-008-9169-0.
26. Zeisberg M, Neilson EG. Biomarkers for epithelial-mesenchymal transitions. J Clin Investig. 2009;119(6):1429–37. https://doi.org/10.1172/JCI36183.